RADIOMETRIC CALIBRATION OF FENGYUN-3D MERSI-II SATELLITE: A CASE STUDY IN LAKE QINGHAI, CHINA

Lin Yan[1,2], Yonghong Hu[2], Xiaoming Li[2], Jun Li[1], Yong Zhang[3], Changyong Dou[2], Javier Plaza[4], Antonio Plaza[4]

[1]School of Geography and Planning, Sun Yat-sen University, Guangzhou 510275, China
[2]Institute of Remote Sensing and Digital Earth, Chinese Academy of Sciences Beijing 100094, China
[3]National Satellite Meteorological Center, Beijing 100081, China
[4]Hyperspectral Computing Laboratory, University of Extremadura, 10003 Caceres, Spain

IGARSS 2020 - 2020 IEEE International Geoscience and Remote Sensing Symposium | 978-1-7281-6374-1/20/$31.00 ©2020 IEEE | DOI: 10.1109/IGARSS39084.2020.9323973

ABSTRACT

In this paper, we describe a method for radiometric calibration of Fengyun-3D (FY-3D) MERSI-II TIR, bands 24 and 25 that combines vicarious and cross-calibration of the corresponding bands of Aqua MODIS, bands 31 and 32. A field campaign was conducted on lake Qinghai, China, on August 18, 2019. The surface measurements were performed before and after the passing time of Terra MODIS and FY-3D MERSI-II. Path radiance and transmittance were then calculated via the radiative transfer code MODTRAN 4.0, and the difference caused by the relative spectral response (RSR) of the sensors was eliminated by the spectral matching. Our experimental results indicate that the obtained radiometric calibration accuracy of FY-3D MERSI-II is stable during on-orbit operation.

Index Terms— Vicarious calibration, MODIS, FY-3D MERSI-II, cross-calibration.

1. INTRODUCTION

Thermal infrared channels provide information about Earth emission radiation, which plays an important role in cloud detection, surface temperature inversion, and heat budget. The radiometric calibration accuracy of satellite sensors changes with the degradation of the performance of their detectors, and also by the influence of outer space environment [1]. Therefore, it is essential to assess the status of satellite sensors during their on-orbit operations.

Vicarious calibration is an important approach to perform radiometric calibration of satellite sensors when the satellite is on-orbit. Different targets, such as deserts [2, 3], deep convective clouds (DCCs) [4, 5], and lakes [6, 7] have been used to perform radiometric calibration between satellite sensors. Lakes have proven to be an ideal target for radiometric calibration, especially for thermal infrared (TIR) sensors. Lake Qinghai is an important China radiometric calibration sites (CRCS) for TIR sensors. Due to its characteristics (large area, flat, and homogeneous), Qinghai Lake has been used since the 1990s to calibrate many satellite sensors in China, i.e., the Fengyun (FY) series [6, 7], the Huanjing (HJ) series [8], or the China-Brazil Earth resources (CBERS) series [9, 10].

In this paper, we describe a method for radiometric calibration accuracy of FY-3D MERSI-II. A field campaign was conducted from Aug 16, 2019 to Aug 22, 2019 at Lake Qinghai to support our methodology. The radiometric calibration of FY-3D MERSI-II TIR bands 24, 25 was performed through the vicarious and cross-calibration of the corresponding bands of Aqua MODIS, bands 31, 32, respectively. Our results confirm stable calibration accuracy of FY-3D MERSI-II during on-orbit operation.

2. CONSIDERED SATELLITES

2.1. FY-3D MERSI-II

The MERSI-II was launched on November 11, 2017 as the most important payload onboard the FY-3D satellite. An improved version of MERSI, MERSI-II is the first imaging instrument which can acquired infrared data of split-window regions with spatial resolution of 250m around the Earth. Moreover, the MERSI-II captures true color Earth images with 250m spatial resolution without any gaps every day. The MERSI-II has 25 spectral bands and uses detectors located on the focal plane that cover the solar spectrum from 0.412μm to 12.0μm. MERSI-II bands 4-7 and 15-25 cover the solar spectrum from 0.865μm to 12.0μm, producing TIR images, while bands 1-3 and 8-14 (covering 0.470μm to 0.746μm) produce images of visible and near-infrared (VNIR) solar radiation. The MERSI-II TIR bands are calibrated through a full-aperture onboard black-body (BB), space view and the moon, respectively. The specification of absolute radiometric accuracy for MERSI-II TIR band is 05K@270K.

This work was supported by National Key Research and Development Program of China under Grant 2017YFB0502900, Special Program for Strategic Leading Science and Technology of Chinese Academy of Sciences (Class A) XDA19010402, Hunan Provincial Key Research and Development Program of China under Grant 2019SK2102.

2.2. Terra MODIS

MODIS (aboard the Terra satellite) was launched on 18 December, 1999. The MODIS sensor has 36 spectral bands and uses detectors located on the focal plane that cover the solar spectrum from 0.412μm to 14.4μm. MODIS bands 1-19 (covering from 0.412μm to 2.1μm) produce images of daytime solar radiation, while bands 20-25 and 27-36 (covering from 3.7μm to 14.4μm) collect thermal images which provide daytime and nighttime observation of Earth. The MODIS solar reflective bands are calibrated by on-orbit calibrators, including a solar diffuser and a solar diffuser stability monitor, whereas the thermal bands are calibrated by an on-orbit BB. The spatial resolution of MODIS bands 1 and 2 is 250 m. The resolution of bands 3 and 4 is 500m, while the resolution of bands 5-36 is 1000m.

3. PROPOSED METHOD

3.1. Theory

The at-sensor radiance measured by the FY-3D MERSI-II satellite at TIR bands contains three parts: i) the radiance reflected from the target after the interaction with the atmosphere, ii) the radiance scattered from the atmosphere itself, and iii) the radiance emitted from the target after the attenuation by the atmosphere. Hence, the radiance received by the sensor can be modeled as follows:

$$L_s(\lambda) = \tau_\alpha(\lambda)L_t(\lambda) + L_{path}(\lambda) + \tau_\alpha(\lambda)L_d(\lambda)\rho_e(\lambda), \quad (1)$$

where $L_s(\lambda)$ is the spectral radiance received by the sensor, $\tau_\alpha(\lambda)$ is the spectral transmittance of the atmosphere, $L_{path}(\lambda)$ is the path radiance scattered from the atmosphere, $L_d(\lambda)$ is the radiance emitted by the target, and $\rho_e(\lambda)$ is the surface emissivity. In our work, the spectral transmittance $\tau_\alpha(\lambda)$ and the path radiance, L_{path} were calculated with MODTRAN 4.0 using simultaneous measurements when the FY-3D MERSI-II overpassed Lake Qinghai on Aug. 18, 2019.

3.2. Spectral Matching

The difference between the relative spectral response (RSR) of the satellite sensors when performing cross-calibration should be eliminated, because they can result in different radiance or reflectance (even if they are observing the same target at the same time). Ratios such as spectral band adjustment factor (SBAF), and matched-image adjustment factor (MIAF) are applied to reduce mismatches between RSRs based on the measured or simulated hyperspectral radiance or reflectance profile of the target, i.e., the MODTRAN simulated radiance (or reflectance) profile [11, 12]:

$$\rho_{\mathrm{MO}} = \frac{\int \mathrm{RSR}_{\mathrm{MO}}(\lambda)\rho(\lambda)d\lambda}{\int \mathrm{RSR}_{\mathrm{MO}}(\lambda)d\lambda}, \quad (2)$$

$$\rho_{\mathrm{ME}} = \frac{\int \mathrm{RSR}_{\mathrm{ME}}(\lambda)\rho(\lambda)d\lambda}{\int \mathrm{RSR}_{\mathrm{ME}}(\lambda)d\lambda}, \quad (3)$$

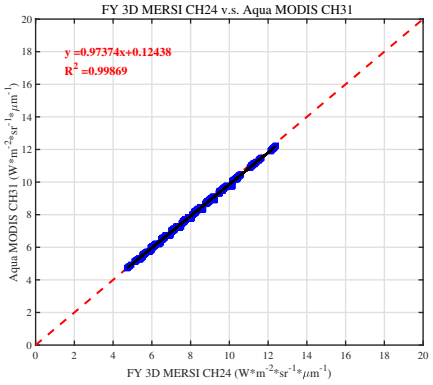

Fig. 1. Spectral matching result between FY-3D MERSI-II band 24 and Aqua MODIS band 31.

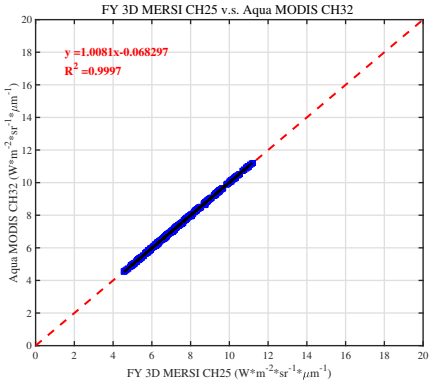

Fig. 2. Spectral matching result between FY-3D MERSI-II band 25 and Aqua MODIS band 32.

where ρ_{MO} and ρ_{ME} are the simulated top-of-atmosphere (TOA) reflectance of MODIS and MERSI-II, respectively. RSR_{MO} and RSR_{ME} respectively represent the relative spectral response (RSR) of MODIS and MERSI-II. $\rho(\lambda)$ is the TOA reflectance profile simulated by MODTRAN 4.0. Due to the lack of a hyperspectral emissivity profile of Lake Qinghai, SBAF or MIAF are not suitable for spectral matching between the CE312, FY-3D MERSI-II and Aqua MODIS. Hence, in this work, the $\rho(\lambda)$ is calculated based on six built-in atmosphere profiles (i.e., tropical, mid-latitude summer/winter, sub-arctic summer/winter included in 1976 U.S. Standard), two observing geometries (vertical and 10°), and nine temperature scenarios (278K, 283K, 288K, 293K, 298K, 303K, 208K, 212K, 320K) via the MODTRAN 4.0. Linear fitting was performed once the simulated TOA reflectance was calculated for the two sensors. Fig. 1 and Fig. 2 respectively show the spectral matching results for MERSI-II bands 24 and 25 with the corresponding bands of MODIS.

Table 1. Input parameters of MODTRAN4.0 for path radiance and transmittance calculation.

Sensor	FY-3D MERSI-II
Date	2019/08/18
Overpassing Time (UTC)	06:34:00
Solar Zenith (°)	28.4740
Solar Azimuth (°)	219.2028
Satellite Zenith (°)	21.3344
Satellite Azimuth (°)	261.5048.00
Ground Altitude (km)	2.360
AOD@550nm	0.360

As we can see from these figures, the MERSI-II simulated TOA reflectance is in good agreement with that of MODIS in the corresponding TIR bands.

3.3. Method

Our methodology for calibration of FY-3D MERSI-II TIR, bands 24 and 25 combines vicarious and cross-calibration based on Aqua MODIS. Fig. 3 shows the flowchart of our calibration strategy for FY-3D MERSI-II TIR bands. The vicarious calibration is based on simultaneous measurements during overpasses of FY-3D, including surface temperature, aerosol optical depth (AOD) and atmospheric profiles.

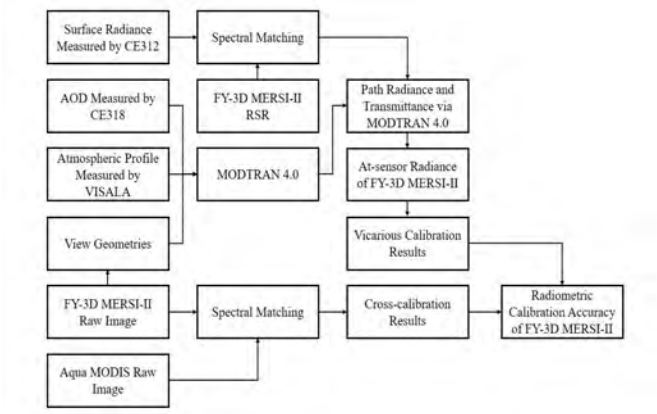

Fig. 3. Flowchart of the proposed calibration method.

4. RESULTS

4.1. Surface Measurements

One of the most important aspects in our vicarious calibration process is the measurement of the surface temperature of lake Qinghai. In our ground campaign, the surface temperature was measured by the CE312 IR radiometer (the benchmark precision instrument for measurements of spectral luminance in 4 to 6 thermal infra-red bands) after rigorous laboratory calibration. Two bands of CE312, i.e., those at 10.8 and 12.0 microns, were used to match the corresponding bands of FY-3D MERSI-II and Aqua MODIS, respectively. During the overpass of the satellite sensors, the CE312 was attached to an unmanned boat about 1.5m from the surface of the lake.

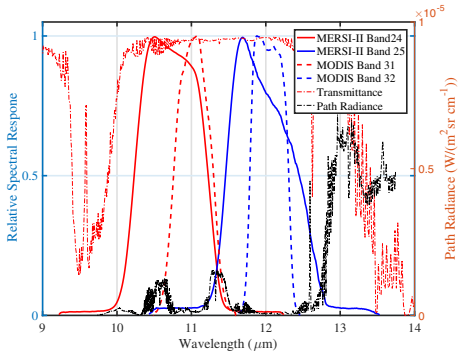

Fig. 4. Path radiance of FY-3D MERSI-II and Terra MODIS on Aug. 18.

Moreover, an atmospheric profile was measured by a radiosonde equipment located near the shore of Lake Qinghai. The balloon, manufactured by the VAISALA, was released to measure the vertical temperature, relative humidity, and pressure one hour before the overpass of FY-3D MERSI-II. The aerosol optical depth (AOD) was measured simultaneously at the same location where the radiosonde balloon was released. The input parameters of MODTRAN 4.0 for path radiance and transmittance calculation are listed in Table 1. Fig. 4 shows the simulated profiles of path radiance and transmittance, along with the RSR of the corresponding bands.

4.2. Calibration Results

Table 2 shows the obtained calibration results based on the simultaneous measurements conducted on Aug. 18, 2019. As we can see from Table 2, the differences for FY-3D MERSI-II are -0.2631K for band 24, and -0.4.000K for band 25, respectively. However, the results of the cross-calibration for these two corresponding bands are -2.5663K, and 2.9027K, respectively. Compared with the vicarious calibration, such large difference in cross-calibration may be caused by the sharpen variation of atmosphere in the overpassing time of MERSI-II and MODIS. Hence, our results combining vicarious calibration and cross-calibration exhibit the potential to achieve stable calibration accuracy of FY-3D MERSI-II during on-orbit operation.

5. CONCLUSIONS

In this paper, we present a new method for calibration of FY-3D MERSI-II satellite that combines vicarious calibration (based on simultaneous measurement results during a field campaign) and cross-calibration via Aqua MODIS. The field

Table 2. Obtained calibration results.

Vicarious calibration results					
Band	**Rad_Raw[1]**	**Rad_Vic[2]**	**BT_Raw[3](K)**	**BT_Sim[4](K)**	**Diff (K)**
MERSI-II Band 24	8.1794	8.2373	290.7020	289.9969	0.2631
MERSI-II Band 25	7.5515	7.5439	289.6797	288.9885	0.4000
Cross-calibration result.					
Band	**Rad_Raw**	**Rad_Coss[5]**	**BT_Raw (K)**	**BT_Sim (K)**	**Diff (K)**
MERSI-II Band 24	8.1794	8.5206	290.7020	293.2683	2.5663
MERSI-II Band 25	7.5515	7.2369	289.6797	286.7770	-2.9027

[1] Radiance calculated from the raw image.
[2] Radiance calculated from vicarious calibration.
[3] Bright temperature calculated from the raw image.
[4] Bright temperature calculated from radiometric calibration.
[5] Radiance calculated from cross-calibration.

campaign was conducted on lake Qinghai, China, to evaluate the radiometric calibration accuracy of FY-3D MERSI-II from Aug. 16, 2019 to Aug. 22, 2019. Surface measurements, including surface temperature, AOD and atmospheric profiles were input to MODTRAN 4.0 to generate the path radiance and transmittance when the FY-3D MERSI-II overpassed lake Qinghai. Moreover, the RSR mismatches between the corresponding bands of CE312, MERSI-II, and MODIS were reduced by linear fitting by means of simulations under different scenarios. The results obtained by combining vicarious calibration and cross-calibration indicate that the obtained calibration accuracy results of FY-3D MERSI-II are stable during on-orbit calibration.

6. REFERENCES

[1] Zhang Yong, *Study on Thermal Infrared Remote Sensors Absolutely Radiometric Calibrations*, Ph.D. thesis, Institute of Remote Sensing and Digital Earth, Chinese Academy of Sciences, 2006.

[2] Akihiko Kuze, D. M. O'Brien, T. E. Taylor, Jason O. Day, and Hiroshi Suto, "Vicarious Calibration of the GOSAT Sensors Using the Railroad Valley Desert Playa," *IEEE Transactions on Geoscience and Remote Sensing*, vol. 49, no. 5, pp. 1781–1795, 2011.

[3] Fumie Kataoka, Robert O. Knuteson, Akihiko Kuze, Hiroshi Suto, Kei Shiomi, Masatomo Harada, Elise M. Garms, Jacola A. Roman, David C. Tobin, and Joe K. Taylor, "TIR Spectral Radiance Calibration of the GOSAT Satellite Borne TANSO-FTS With the Aircraft-Based S-HIS and the Ground-Based S-AERI at the Railroad Valley Desert Playa," *IEEE Transactions on Geoscience and Remote Sensing*, vol. 52, no. 1, pp. 89–105, 2014.

[4] Wenhui Wang and Changyong Cao, "Assessing the VIIRS RSB Calibration Stability Using Deep Convective Clouds," *Proceedings of SPIE - The International Society for Optical Engineering*, vol. 9264, no. 10, 2014.

[5] Wenhui Wang and Cao Changyong, "Monitoring the NOAA Operational VIIRS RSB and DNB Calibration Stability Using Monthly and Semi-Monthly Deep Convective Clouds Time Series," *Remote Sensing*, vol. 8, no. 1, pp. 32–51, 2016.

[6] Yong Zhang, Zhaojun Zheng, Xiuqing Hu, Zhiguo Rong, and Lijun Zhang, "Lake Qinghai: Chinese site for radiometric calibration of satellite infrared remote sensors," *Remote Sensing Letters*, vol. 4, no. 4, pp. 315–324, 2012.

[7] Jinjun Tong, S. J. Dry, Yun Chen, and Bo Hu, "An alternative method for in-flight absolute radiometric calibration of thermal infrared channels of chinese geostationary meteorological satellites," *International Journal of Remote Sensing*, vol. 31, no. 3, pp. 791–803, 2010.

[8] L. Liu, X. Gu, T. Yu, X. Li, and T. Shi, "HJ-1B thermal infrared band in-flight radiometric calibration and validation," *Infrared and Laser Engineering*, vol. 41, no. 5, pp. 1119–1125, 2012.

[9] Yong Zhang, Xingfa Gu, and Yu Tao, "In-flight method for CBERS-02 IRMSS thermal channel absolute radiometric calibration at Lake Qinghai (China)," IEEE International Geoscience and Remote Sensing Symposium 2005, 2005.

[10] Yong Zhang, Xingfa Gu, and Yu Tao, "Radiometric Cross-Calibration of CBERS-02 IRMSS Thermal Channel," *Journal of Infrared and Millimeter Waves*, vol. 25, no. 4, pp. 261–266, 2006.

[11] Gyanesh Chander, Nischal Mishra, Dennis L. Helder, David B. Aaron, Amit Angal, Taeyoung Choi, Xiaoxiong Xiong, and David R. Doelling, "Applications of Spectral Band Adjustment Factors (SBAF) for Cross-Calibration," *IEEE Transactions on Geoscience and Remote Sensing*, vol. 51, no. 3, pp. 1267–1281, 2013.

[12] Hailiang Gao, Xingfa Gu, Yu Tao, Sun Yuan, and Qiyue Liu, "Cross-Calibration of GF-1 PMS Sensor With Landsat 8 OLI and Terra MODIS," *IEEE Transactions on Geoscience and Remote Sensing*, vol. 54, no. 8, pp. 1–8, 2016.